

Improved limits on the hadronic and semi-hadronic CP violating parameters and role of a dark force carrier in the electric dipole moment of ^{199}Hg

B. K. Sahoo *

Physical Research Laboratory, Navrangpura, Ahmedabad-380009, India

(Dated: Received date; Accepted date)

Combining the recently reported electric dipole moment (EDM) of ^{199}Hg atom due to breaking of parity and time-reversal symmetries with the improved relativistic atomic calculations, precise limits on the tensor-pseudotensor (T-PT) electron-nucleus (e-N) coupling coefficient and the nuclear Schiff moment (NSM) interactions are determined. Using these limits with the nuclear calculations, we infer limits on the EDMs of neutron and proton as $d_n < 2.2 \times 10^{-26} |e|\text{cm}$ and $d_p < 2.1 \times 10^{-25} |e|\text{cm}$, respectively, and on the quantum chromodynamics (QCD) parameter and the combined up- and down- quark chromo-EDMs as $|\bar{\theta}| < 1.1 \times 10^{-10}$ and $|\tilde{d}_u - \tilde{d}_d| < 5.5 \times 10^{-27} |e|\text{cm}$, respectively. These are the best limits till date to probe new sources of CP violation beyond the standard model (SM) from a diamagnetic atom. Role of considering a capable many-body method to account the electron correlation effects to all orders for inferring the above limits has been highlighted. From this analysis, constraints on the T-PT e-N coupling coefficient with a large range of mass of a possible dark matter carrier χ between the atomic electrons and nucleus are given.

PACS numbers: 21.10.Ky, 31.15.aj, 31.30.Gs, 32.10.Fn

I. INTRODUCTION

Observation of permanent electric dipole moment (EDM) in a non-degenerate physical system like an atom is a signature of violations of parity (P) and time-reversal (T) symmetries [1–3]. As a consequence of CPT theorem [4], T violation implies violation of combined charge conjugation (C) and P symmetries (CP violation). On many counts, investigating CP violation is a subject of fundamental importance [5, 6], which motivates to study CP violating interactions extensively on many different systems [7–11]. It has so far been observed only in the K [12] and B mesons [13–15] at the elementary particles level and the results of these experiments are in agreement with the predictions of the Standard Model (SM). CP-violation in the SM arises through a complex phase parameter, δ , of the Cabibbo-Kobayashi-Maskawa (CKM) matrix, and due to the P,T-odd interactions between the quarks and gluons characterized by the quantum chromodynamics (QCD) parameter θ [16–18]. But the amount of CP violation described by the SM are not sufficient to explain the observed finiteness of neutrino masses, the matter-antimatter asymmetry in the Universe, the existence of dark matter etc. [19, 20]. To answer to these profound fundamental questions, many extensions of the SM, like the multi-Higgs, supersymmetry, left-right symmetric etc. models have been propounded in the literature [17, 18, 21]. Direct probe of new sources of CP violations to plausibly explain many of the above beyond SM (BSM) physics can only be carried out at very high energy scale, but it is beyond the reach of the presently operating accelerator facilities like large hadron collider (LHC). Therefore, it is imperative to obtain model in-

dependent CP violating parameters through indirect approaches to validate models supporting the BSM physics [17, 18]. In this context, inferring precise limits on CP violating parameters from the electric dipole moments (EDMs) of composite systems such as atoms can be very useful.

Elementary particles such as electrons and quarks can acquire finite dimensions due to CP violating interactions [17, 21]. These dimensions can be estimated from the knowledge of EDMs of the respective particles. SM predicts very small EDMs of electrons and quarks [18, 21], but many popular BSM models such as theories like minimal supersymmetric extension of the SM and weak scale supersymmetry model (two variants of supersymmetry), multi-Higgs model, two-loop radiative correction to SM etc. [17, 18, 22–24] predict numerous amount of CP violation. Similarly, the coupling coefficients of the CP violating interactions between these elementary particles are estimated to be larger in these models than the SM. The effects due to EDMs of the constituent particles and CP violating interactions among the electrons and quarks are enhanced enormously in the atoms and molecules due to the relativistic and correlation effects observed by the bound electrons [16, 25, 26]. This makes atoms and molecules are the paramount platforms for investigating CP violating effects arising due to BSM. By combining measured EDMs of atoms or molecules with the corresponding calculations it is possible to infer information on the EDMs of the electron and quarks and model independent electron-quark (e-q) CP violating coupling coefficients from the electron-nucleus (e-N) coupling coefficients deducing them via the electron-nucleon (e-n) couplings [26]. Categorically, atoms or molecules with the open-shell structure (paramagnetic systems) are sensitive to dominant contributions from the electron EDM (d_e) and the pseudoscalar-scalar (PS-S) contribution from the CP violating e-N interactions while the closed-shell (dia-

*Email: bijaya@prl.res.in

magnetic) atomic systems are the suitable candidates for probing chromo-EDMs of up (\tilde{d}_u) and down (\tilde{d}_d) quarks, extracting values of the θ parameter, the tensor-pseudotensor (T-PT) and scalar-pseudoscalar (S-PS) CP violating coupling e-q coefficients etc. In this work, we intend to investigate EDM of the ^{199}Hg diamagnetic atom to estimate precise limits on different CP violating parameters, which arises predominantly due to the nuclear Schiff moment (NSM) [26] and the T-PT and S-PS e-N interactions [17, 27]. The former is associated with the CP violating nucleon-nucleon (n-n) interactions or the EDMs of the proton (d_p) and the neutron (d_n), which in turn originates from the CP violating quark-quark (q-q) interactions as well as EDMs (d_q) and chromo-EDMs (\tilde{d}_q) of the quarks at the elementary particle level [18, 24, 28], while the later comes from the CP violating e-q interactions.

Though there has not been observation of finite EDM in any system till today, but the on-going atomic and sub-atomic experiments are continuously improving limits on the EDMs of neutron [29], atoms [10, 11] and molecules [8, 9]. Enhancements of P,T-odd interactions in atoms and molecules are larger than neutron with respect to the fundamental particles. Molecules are the better candidates for finding out more precise limit on d_e owing to strong polarization effects exhibited within the paramagnetic polar molecules that produce large internal electric fields and causes large energy shifts in the molecular energy levels than the atomic energy levels when d_e of the valence electron interacts with an external electric field. However, consideration of diamagnetic atoms than diamagnetic molecules are advantageous for studying the NSM and T-PT e-N interactions as atomic systems involve comparatively simpler nuclear interactions than molecules. It to be noted that for deducing e-q interaction coefficients from the e-N interactions, accurate knowledge of nuclear interactions are also essential [24, 26, 28]. So far, measurements only in the ^{129}Xe [30], ^{199}Hg [10, 31] and ^{225}Ra [11, 32] diamagnetic atoms have been performed among which the EDM of the ^{199}Hg atom is reported more precisely from a recent measurement as $d(^{199}\text{Hg}) = (-2.20 \pm 2.75(\text{stat}) \pm 1.48(\text{sys})) \times 10^{-30}$ ecm corresponding to an upper limit $|d(^{199}\text{Hg})| < 7.4 \times 10^{-30}$ ecm with 95% confidence level [10]. In our previous work [33], we had obtained limits on θ and $|\tilde{d}_u - \tilde{d}_d|$ by combining atomic calculations, carried out by employing a relativistic coupled-cluster (RCC) method, with the measurement on EDM of ^{199}Hg reported earlier in Ref. [31]. We had also demonstrated in that work that other relativistic methods such as random phase approximation (RPA) estimate very large magnitudes of atomic results for neglecting some of the important electron correlation effects like pair-correlation effects. Hence, use of those calculations give rise much lower limits on the above quantities. We attempt to review these limits here by considering the latest experimental data from Ref. [10] and embodying more contributions in the atomic calculations from higher order electron correlations, espe-

TABLE I: Calculated α_d value in $|e|a_0^2$ and d_a values with the T-PT e-N interaction (given in $10^{-20} C_T \langle \sigma_N \rangle |e|\text{cm}$) with $m_\chi = \infty$ and nuclear Fermi charge distribution and the NSM interaction (given in $(10^{-17} [S/|e|fm^3] |e|\text{cm})$ in the ^{199}Hg atom from the DHF, MBPT(2), MBPT(3), RPA and CCSD methods. Good agreement between the experimental and CCSD values of α_d suggests, CCSD method is capable of producing more accurate results.

Method	α_d	T-PT	NSM
DF	40.95	-2.39	-1.20
MBPT(2)	34.18	-4.48	-2.30
MBPT(3)	22.98	-3.33	-1.72
RPA	44.98	-5.89	-2.94
CCSD	34.51	-3.17	-1.76
Experiment [41]	33.91(34)		

cially from the pair-correlation effects, through the RCC method. Moreover, the required nuclear calculations have also been revised extensively all along [34, 35].

In fact, observation of dark matter in the universe has unearthed another Pandora's box to study interactions among the particles in their presence. It is believed that matters could interact with each other in the presence of dark forces by exchanging gauge boson types of particles, known as dark force carriers, possessing very weak couplings. It is again strenuous to observe these effects through the accelerator based methods, even though their masses can be of reasonable size, because of their exceptionally smaller cross-sections. In a recent work [36], the P,T-odd interaction between the electrons and nucleons in ^{199}Hg due to the exchange of a massive light gauge boson χ was investigated and constraint on the T-PT e-N coupling constant with a range of mass of χ (m_χ) was given. In that study, the previously measured experimental data on ^{199}Hg EDM from Ref. [31] was used, which has now been improved almost by one order very recently [10], and a relativistic RPA method, accounting only the core-polarization effects of electron correlations, was employed to estimate the T-PT interaction enhancement due to the exchange of χ between the electrons and nucleus in this atom. We improve accuracies in the atomic calculations further using the RCC method and use the latest experimental result to put more stringent limit on the T-PT e-N coupling constant.

In order to ascertain validity of the employed methods in the present study, we also perform calculation of the dipole polarizability (α_d) of Hg atom, which has similar expression for evaluating the P,T-odd interactions, using the considered many-body methods and compare the results with the available experimental value.

II. THEORETICAL FORMALISM

The P,T-odd Lagrangian for the e-n interaction is given by [18]

$$\mathcal{L}_{e-n}^{PT} = C_T^{e-n} \varepsilon_{\mu\nu\alpha\beta} \bar{\psi}_e \sigma^{\mu\nu} \psi_e \bar{\psi}_n \sigma^{\alpha\beta} \psi_n + C_P^{e-n} \bar{\psi}_e \psi_e \bar{\psi}_n i \gamma_5 \psi_n, \quad (1)$$

where $\varepsilon_{\mu\nu\alpha\beta}$ is the Levi-Civita symbol and $\sigma_{\mu\nu} = \frac{i}{2}[\gamma_\mu, \gamma_\nu]$ with the γ 's being the Dirac matrices. C_T^{e-n} and C_P^{e-n} are the T-PT and S-PS e-n interaction coupling constants respectively. Here ψ_n and ψ_e represent the Dirac wave functions of the nucleon and electron respectively. Assuming that the T-PT and S-PS e-N interactions act independently, we can consider them individually in the atomic calculations for which the respective e-N interaction Hamiltonians are given as [26, 27, 38]

$$H_{e-N}^{TPT} = i\sqrt{2}G_F C_T \sum_e \boldsymbol{\sigma}_N \cdot \boldsymbol{\gamma} \rho_N(r) \quad (2)$$

and

$$H_{e-N}^{SPS} = -\frac{G_F}{\sqrt{2}m_n c} C_P \sum_e \gamma_0 \boldsymbol{\sigma}_N \cdot \boldsymbol{\nabla} \rho_N(r), \quad (3)$$

where G_F is the Fermi constant, C_T and C_P are the T-PT and S-PS e-N coupling constants, $\boldsymbol{\sigma}_N = \langle \boldsymbol{\sigma}_N \rangle \mathbf{I}/I$ is the Pauli spinor of the nucleus with spin I , $\rho_N(r)$ is the nuclear density, m_n is the nucleon mass and c is the speed of light. C_P can be estimated with reasonable accuracy from the knowledge of C_T using an empirical relation [26, 38]

$$C_P \approx 3.8 \times 10^3 \times \frac{A^{1/3}}{Z} C_T \quad (4)$$

with the atomic number Z and mass A . We are only interested in determining the C_T value here so that C_P can be estimated using the above relation.

The Lagrangian for the P,T-odd pion-nucleon-nucleon (π -n-n) interaction that also contribute predominantly to the EDMs of the diamagnetic atoms is given by [18]

$$\mathcal{L}_{e-n}^{\pi nn} = \bar{g}_0 \bar{\psi}_n \tau^i \psi_n \pi^i + \bar{g}_1 \bar{\psi}_n \psi_n \pi^0 + \bar{g}_2 (\bar{\psi}_n \tau^i \psi_n \pi^i - 3 \bar{\psi}_n \tau^3 \psi_n \pi^0) \quad (5)$$

where the couplings \bar{g}_i with the superscript $i = 1, 2, 3$ represent the isospin components. The corresponding e-N interaction Hamiltonian is given by [26, 38]

$$H_{e-N}^{NSM} = \frac{3\mathbf{S} \cdot \mathbf{r}}{B_4} \rho_N(r), \quad (6)$$

where $\mathbf{S} = S \frac{\mathbf{I}}{2}$ is the NSM and $B_4 = \int_0^\infty dr r^4 \rho_N(r)$. The magnitude of the NSM S can be expressed as [24, 26]

$$S = g_{\pi nn} \times (a_0 \bar{g}_{\pi nn}^{(0)} + a_1 \bar{g}_{\pi nn}^{(1)} + a_2 \bar{g}_{\pi nn}^{(2)}), \quad (7)$$

where $g_{\pi nn} \simeq 13.5$ is the CP-even π -n-n coupling constant, a_i s are the polarizations of the nuclear charge distribution that can be computed to reasonably accuracy

using the Skyrme effective interactions in the Hartree-Fock-Bogoliubov mean-field method [24] and $\bar{g}_{\pi nn}^{(i)}$ s with $i = 1, 2, 3$ representing the isospin components of the CP-odd π -n-n coupling constants. These couplings are related to \tilde{d}_u and \tilde{d}_d as $\bar{g}_{\pi nn}^{(1)} \approx 2 \times 10^{-12} \times (\tilde{d}_u - \tilde{d}_d)$ [18, 23, 35] and $\bar{g}_{\pi nn}^{(0)}/\bar{g}_{\pi nn}^{(1)} \approx 0.2 \times (\tilde{d}_u + \tilde{d}_d)/(\tilde{d}_u - \tilde{d}_d)$ [18, 34], where chromo-EDMs of quarks are scaled with $\times 10^{-26} |e| \text{cm}$. It is also related to $\bar{\theta}$ parameter by $|\bar{g}_{\pi nn}^{(1)}| = 0.018(7) \bar{\theta}$ [34]. From the nuclear calculations, one can obtain $S \simeq (1.9d_n + 0.2d_p) \text{ fm}^2$ [28].

Again allowing the exchange of dark matter gauge boson χ between the electrons and nucleus in the considered atoms, the T-PT e-N interaction Hamiltonian can be expressed by [36]

$$H_{e-N}^{TPT} = i\sqrt{2}G_F C_T^\chi \sum_e \boldsymbol{\sigma}_N \cdot \boldsymbol{\gamma} \rho_N^\chi(r), \quad (8)$$

where C_T^χ and $\rho_N^\chi(r)$ are the corresponding modified T-PT coupling constant and nuclear density, respectively, with the exchange of dark force carrier χ . It to be noted that the above expression is the most general one in describing the contact interaction due to finiteness of the exchange boson m_χ and Eq. (2) can be treated as the special case valid in the limit $m_\chi \rightarrow \infty$. Therefore, it yields $C_T^\chi \xrightarrow{m_\chi \rightarrow \infty} C_T$ and $\rho_N^\chi \xrightarrow{m_\chi \rightarrow \infty} \rho_N$. Owing to this fact, it is needed to define a contact potential of Yukawa-type between the electrons and nucleons in an atom due to exchange of m_χ such as [36]

$$V_\chi(r, r') = \frac{e^{-m_\chi c|\mathbf{r}-\mathbf{r}'|}}{4\pi|\mathbf{r}-\mathbf{r}'|}, \quad (9)$$

where r and r' represent coordinates of the electrons and the nucleons respectively. It can be shown that in the large mass limit, this Yukawa-type potential behaves like $\delta^3(r - r')/(m_\chi c)^2$. Considering this potential, $\rho_N^\chi(r)$ is given by [36]

$$\rho_N^\chi(r) = 4\pi(m_\chi c)^2 \int dr' V_\chi(r, r') \rho_N(r'). \quad (10)$$

For convenient determination of $V_\chi(r, r')$, uniform charge density of the nucleus is taken into account in which we define

$$\rho_N(r) = \rho_0 \Theta(1 - (r/R)), \quad (11)$$

with $\rho_0 = \frac{3Z}{4\pi R^3}$ for the radius of the sphere R within which the nucleons are uniformly distributed and Θ is the Heaviside step function. Using this approximation, it yields [36]

$$\rho_N^\chi(r) = \rho_0 \frac{\lambda_\chi}{r} \begin{cases} \frac{r}{\lambda_\chi} - e^{-\frac{r}{\lambda_\chi}} \left(1 + \frac{R}{\lambda_\chi}\right) \sinh\left(\frac{r}{\lambda_\chi}\right), & r \leq R \\ e^{-\frac{r}{\lambda_\chi}} \left(\frac{R}{\lambda_\chi} \cosh\left(\frac{R}{\lambda_\chi}\right) - \sinh\left(\frac{R}{\lambda_\chi}\right)\right), & r > R, \end{cases} \quad (12)$$

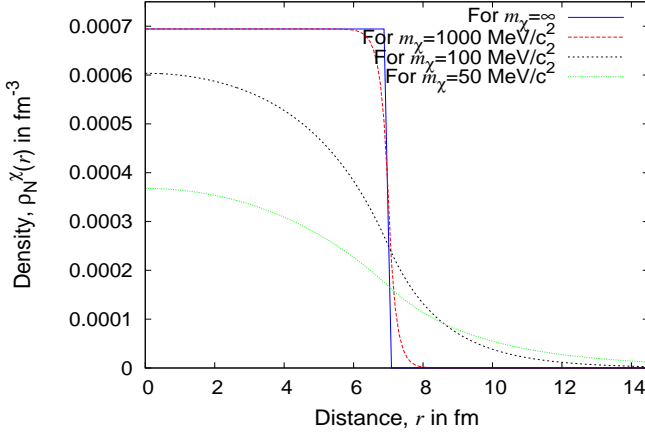


FIG. 1: (Color online) Behavior of ρ_N^χ values with the distance from the origin of the nucleus of ^{199}Hg in the uniform charge distribution for different values of m_χ (in MeV/c^2). This is perfectly in agreement with the findings of Ref. [36].

where $\lambda_\chi = \hbar/(m_\chi c)$. As can be seen this density functional goes as $\rho_N^\chi(r) \propto \frac{e^{-r/\lambda_\chi}}{r}$. In order to demonstrate the validity of considering nuclear uniform charge distribution in our EDM calculation, we also compare the values with the result obtained by considering the nuclear Fermi charge density distribution for the limit $m_\chi \rightarrow \infty$ as

$$\rho_N(r) = \frac{\rho_0}{1 + e^{(r-b)/a}}, \quad (13)$$

where ρ_0 is the corresponding normalization constant, b is the half-charge radius and $a = 2.3/4(\ln 3)$ is related to the skin thickness.

Denoting d_a^χ and d_a^c are the EDM of the atom due to exchange of finite mass of m_χ (due to contact interaction) and with infinite mass of m_χ respectively, we can express a ratio as

$$\mathcal{R}^\chi = \frac{d_a^\chi/C_T^\chi}{d_a^c/C_T^c}, \quad (14)$$

so that it follows

$$d_a^\chi \equiv C_T^\chi \left(\frac{d_a^c}{C_T^c} \right) \mathcal{R}^\chi \leq \text{Measured EDM of the atom.} \quad (15)$$

Thus, using the experimental EDM value of ^{199}Hg we can express

$$|C_T^\chi| \leq |d(^{199}\text{Hg})| \left| \frac{C_T}{d_a^c} \frac{1}{\mathcal{R}^\chi} \right|. \quad (16)$$

By calculating $\frac{C_T}{d_a^c}$ for infinite value of m_χ and \mathcal{R}^χ for a wide range of m_χ , we shall be able to constraint on C_T^χ using the experimental value of $d(^{199}\text{Hg})$. For this purpose, it is necessary to evaluate $\frac{C_T}{d_a^c}$ and \mathcal{R}^χ reliably by employing potential relativistic atomic many-body theories such as RPA and RCC methods that are described briefly in the following section.

III. METHOD OF CALCULATIONS

To pursue calculations of atomic wave functions, we start with the mean-field wave function ($|\Phi_0\rangle$) of the ground state

of ^{199}Hg using the Dirac-Hartree-Fock (DHF) method in the Dirac-Coulomb (DC) atomic Hamiltonian. With the reference state $|\Phi_0\rangle$, the ground state ($|\Psi_0\rangle$) is determined by appending the electron correlations in the RPA and RCC methods as described in our previous work [33]. These methods are briefly described below.

Using the RCC method ansatz, we can express [37]

$$|\Psi_0^{(0)}\rangle = e^{T^{(0)}} |\Phi_0\rangle, \quad (17)$$

where $T^{(0)}$ is the even parity RCC operators that takes care of the neglected correlation effects of the DHF method among the electrons to all orders by exciting them to the higher states with respect to $|\Phi_0\rangle$. In the presence of a P,T-odd interaction, this wave function is modified to

$$|\Psi_0\rangle = e^T |\Phi_0\rangle = e^{T^{(0)} + \lambda T^{(1)}}, \quad (18)$$

where $T = T^{(0)} + \lambda T^{(1)}$ accounts both the electron correlation effects due to the electromagnetic interactions by $T^{(0)}$ and electromagnetic interactions along with the P,T-odd weak interaction by $T^{(1)}$ to all orders. Here λ can be interpreted as the strength of the coupling coefficient of the considered P,T-odd interaction. Note that $|\Psi_0\rangle$ becomes a mixed parity state in contrast to the even parity wave function $|\Psi_0^{(0)}\rangle$ owing to addition of the odd-parity P,T-interaction Hamiltonians. Since these weak interactions are much smaller than the electromagnetic interactions in the atoms, we can consider the electron correlation effects to all orders and the P,T-odd interaction to the first order by approximating as

$$|\Psi_0\rangle \simeq |\Psi_0^{(0)}\rangle + \lambda |\Psi_0^{(1)}\rangle, \quad (19)$$

with the corresponding weak coupling coefficient λ which is either C_T^χ or S for the T-PT and NSM interactions, respectively. This yields

$$|\Psi_0^{(1)}\rangle = e^{T^{(0)}} T^{(1)} |\Phi_0\rangle. \quad (20)$$

It implies $|\Psi_0^{(1)}\rangle$ is an odd parity wave function due to $T^{(1)}$. We solve first the amplitudes of the $T^{(0)}$ operators following which we obtain amplitudes of the $T^{(1)}$ operators. For the calculations of both $|\Psi_0^{(0)}\rangle$ and $|\Psi_0^{(1)}\rangle$, we allow only all possible singles and doubles excitations by defining $T^{(0)} = T_1^{(0)} + T_2^{(0)}$ and $T^{(1)} = T_1^{(1)} + T_2^{(1)}$ in the RCC method (CCSD method).

As described in Ref. [33], these wave functions in RPA are given by

$$|\Psi_0^{(0)}\rangle \approx |\Phi_0\rangle \quad \text{and} \quad |\Psi_1^{(0)}\rangle \approx \Omega_I^{(\infty,1)} |\Phi_0\rangle, \quad (21)$$

where $\Omega_I^{(\infty,1)}$ is the RPA excitation operator that accounts only the core-polarization electron correlation effects to all orders and the P,T-odd interaction to one order through the single excitations. As were highlighted in our previous works on similar studies [33, 39, 40], the electron pair-correlation effects contribute significantly to these quantities and cancel out with the core-polarization effects substantially giving rise to smaller values to the final results. Nonetheless, both these core-polarization and pair-correlation effects are being incorporated in the equally footing to all orders and are solved self-consistently using the coupled equations in the RCC method [33, 39, 40].

TABLE II: Variation in the d_a^x values (in $10^{-18} C_T^x \langle \sigma_N \rangle |e|cm$) of ^{199}Hg with m_χ (in MeV/c^2) from the DHF, RPA and CCSD methods with uniform nuclear charge distribution.

m_χ	DHF	RPA	CCSD
∞	-240.33	-591.36	-318.46
4882.81	-238.85	-587.71	-316.49
3906.25	-239.06	-588.22	-316.77
3000.00	-239.15	-588.46	-316.90
2441.41	-239.15	-588.46	-316.90
1953.13	-239.11	-588.35	-316.84
1500.00	-239.03	-588.17	-316.74
976.56	-238.88	-587.80	-316.54
488.28	-238.38	-586.57	-315.88
195.31	-235.40	-579.18	-311.92
97.65	-227.09	-558.80	-300.89
70.0	-219.43	-539.97	-290.72
39.06	-198.95	-489.63	-263.52
19.53	-165.31	-406.98	-218.86
7.81	-115.75	-285.37	-153.01
3.0	-67.80	-168.13	-89.38
1.5625	-40.17	-101.01	-52.93
1.2	-30.70	-78.09	-40.54
1.0	-24.87	-64.02	-32.95
0.9	-21.79	-56.59	-28.96
0.8	-18.62	-48.92	-24.86
0.7	-15.37	-41.07	-20.67
0.6	-12.09	-33.10	-16.46
0.5	-8.85	-25.18	-12.31
0.4	-5.80	-17.56	-8.38
0.3125	-3.45	-11.45	-5.30
0.25	-2.07	-7.63	-3.44
0.2	-1.22	-5.02	-2.22
0.15	-0.62	-2.91	-1.26
0.1	-0.27	-1.34	-0.59
0.0625	-0.13	-0.56	-0.26
0.0125	-0.01	-0.03	-0.02
0.0025	-6.0×10^{-5}	-1.2×10^{-3}	-6.0×10^{-4}
0.00125	1.1×10^{-5}	-2.4×10^{-4}	-1.3×10^{-4}
0.0008	8.0×10^{-6}	-8.0×10^{-5}	-5.4×10^{-5}

After obtaining the $|\Psi_0^{(0)}\rangle$ and $|\Psi_0^{(1)}\rangle$ wave functions in the above formalisms, we evaluate

$$\frac{d_a}{\lambda} \equiv \mathcal{Y} = 2\langle \Psi_0^{(0)} | D | \Psi_0^{(1)} \rangle, \quad (22)$$

for the atomic EDM d_a that corresponds to $\mathcal{Y} = d_a^x / C_T^x$ and $\mathcal{Y} = d_a / S$ for the T-PT and NSM interactions, respectively. This in the RPA is given by

$$\mathcal{Y} = 2\langle \Phi_0 | D \Omega_I^{(\infty,1)} | \Phi_0 \rangle. \quad (23)$$

In the RCC framework, we can obtain [33]

$$\mathcal{Y} = 2\langle \Phi_0 | [e^{T^{(0)\dagger}} D e^{T^{(0)}} T^{(1)}]_{\text{conn}} | \Phi_0 \rangle, \quad (24)$$

where the subscript *conn* implies all the connected terms are evaluated by adopting the Wick's generalized theorem [37]. As can be seen, the above RCC expression has a non-truncative series $e^{T^{(0)\dagger}} D e^{T^{(0)}}$. By replacing the P,T-odd interaction Hamiltonian by a dipole operator D and considering

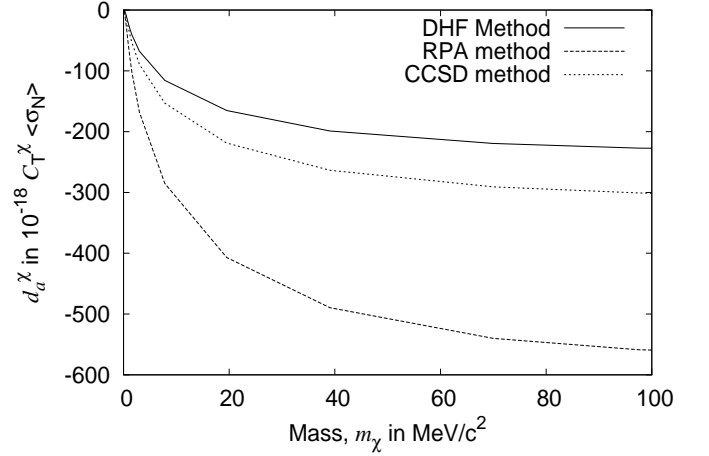


FIG. 2: (Color online) Demonstration of trends in the d_a^x values (in $10^{-18} C_T^x \langle \sigma_N \rangle |e|cm$) with m_χ (in MeV/c^2) from the DHF, RPA and CCSD methods. This clearly shows RPA values are far away from the DHF results, while the CCSD results are close to the DHF values. The differences between the RPA and CCSD results are the clear indication of strong contributions by the electron pair-correlation effects.

$\lambda = 1$ in the evaluation of $|\Psi_0^{(1)}\rangle$, it will give \mathcal{Y} as α_d in the above expressions. As per the generalized Wick's theorem, we break this expression into effective one-body and two-body terms for their evaluations. In our previous work [33], we had demonstrated an approach using which the non-truncative effective one-body terms were calculated self-consistently but contributions from the effective two-body terms were estimated approximately. In this work, we have included more possible effective two-body terms in a self-consistent procedure using the intermediate diagrammatic techniques in the similar manner as discussed in Ref. [37] for accurate evaluation of \mathcal{Y} . These corrections are part of the pair-correlation effects and need to be determined rigorously for attaining more reliable results. Contributions from these diagrams, especially that arise after contracting with the $T_2^{(1)}$ operators, are coming out to be whopping amount and cancel out further with the core-polarization contributions. As a matter of fact, we find the differences between the RPA and CCSD results are quite significant. We also present results considering only one order Coulomb interaction and two orders of Coulomb interactions along with the P,T-odd interaction in the atomic wave function in a perturbative approach of the second order many-body perturbation theory (MBPT(2) method) and the third order many-body perturbation theory (MBPT(3) method) respectively. In our EDM studies on the ^{223}Rn [39] and ^{225}Ra [40] atoms we had demonstrated that the lowest order core-polarization effects enter through the MBPT(2) method while the lowest order pair-correlation effects contribute at the MBPT(3) method. Thus, it is possible to understand about the importance of the pair-correlation contributions from the differences between the results from the MBPT(2) and MBPT(3) methods.

IV. RESULTS AND DISCUSSION

In Table I, we present the d_a values by calculating \mathcal{Y} for the corresponding T-PT e-N and NSM interactions in the ^{199}Hg atom using relativistic many body methods at different levels of the approximations and considering nuclear Fermi charge distribution. The DHF results are obtained using the wave functions from the DHF method. We had already discussed results reported by others employing various many-body methods in our previous work [33]. Here we present the improved CCSD results compared to the values given in Ref. [33] by taking into account the additional effects mentioned in the previous section. In fact, we had already given results from the DHF, MBPT(2), MBPT(3) and RPA methods in Ref. [33] as listed in the above table. However, we present them again here to highlight the reasons for which differences between the RPA and CCSD results occur. This could justify the intention for calculating the C_T^x coupling coefficients due to the exchange of dark matter candidate χ using the CCSD method, which were determined earlier by the RPA method [36]. It is worth mentioning here that our DHF and RPA results given in the above table agree well with another calculation reported in Ref. [38]. Again, α_d values obtained from different methods are given and compared with the experimental result in the same table. As can be seen, the CCSD value $34.51 |e|a_0^2$ is in very good agreement with the experimental value $33.91(34) |e|a_0^2$ [41], while RPA estimates its value far away from the experimental result. The reason for which the CCSD values are coming out to be off from the RPA values can be understood from the differences in the results of the MBPT(2) and MBPT(3) methods. From the computational point of view the DHF and MBPT(2) methods take only less than an hour to produce the results while it takes few hours to perform calculations using the MBPT(3) and RPA methods to obtain the above quantities. However, the bottle-neck of carrying out CCSD calculations is that it takes days to complete a set of results. Thus, the improvements in the results by the CCSD method are done with the cost of huge computational resources.

By combining the \mathcal{Y} values from the CCSD method with the measured EDM of the ^{199}Hg atom reported recently as $|d_a(^{199}\text{Hg})| < 7.4 \times 10^{-30} |e|\text{cm}$ with 95% confidence level [10], we get

$$|C_T| < 7.0 \times 10^{-10} \quad (25)$$

and

$$|S| < 4.2 \times 10^{-13} |e|\text{fm}^3. \quad (26)$$

Here we have used the value $\langle \sigma_N \rangle = -1/3$ of the ^{199}Hg atomic nucleus [38] to deduce the limit on C_T . The above limits are comparatively larger than the estimated limits given in Ref. [33] owing to the fact that consideration of more non-linear effects in the CCSD method gives the corresponding \mathcal{Y} values smaller than the values reported earlier.

From the relation given in Eq. (4), the S-PS e-N coupling coefficient is obtained as

$$|C_P| < 1.9 \times 10^{-7} \quad (27)$$

and from the relation $S \simeq (1.9d_n + 0.2d_p) \text{ fm}^2$ [28], we can get the limit on d_n as

$$|d_n| < 2.2 \times 10^{-26} |e|\text{cm} \quad (28)$$

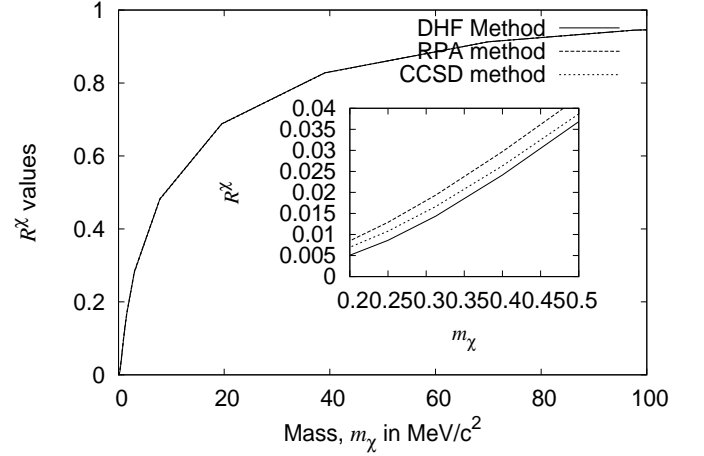


FIG. 3: (Color online) Variation in the R^x values with m_χ (in MeV/c^2) from the DHF, RPA and CCSD methods. We find all the methods are predicting almost same R^x values irrespective of the fact that the trends in the d_a^x results are coming out to be completely different way from all the three employed methods. However, slight deviations in these results can be observed for smaller values of m_χ as shown in the inset of the figure. This observation does not agree perfectly with the findings in Ref. [36] though earlier it was seen that behavior of ρ_N^x was in perfect agreement between both the works.

against the limit $d_n < 3.0 \times 10^{-26} |e|\text{cm}$ obtained from the direct measurement [29] and on d_p as

$$|d_p| < 2.1 \times 10^{-25} |e|\text{cm}. \quad (29)$$

To our knowledge, these are the most reliable limits obtained on d_n and d_p so far.

Based on the discussion in Ref. [34], the tensor component contribution to S from the π -n-n interactions are negligible. With this assumption, it is given as [34]

$$S \simeq [(0.37 \pm 0.3)\bar{g}_{\pi nn}^{(0)} + (0.4 \pm 0.8)\bar{g}_{\pi nn}^{(1)}] |e|\text{fm}^3. \quad (30)$$

From this, we infer the limits

$$|\bar{g}_{\pi nn}^{(0)}| < 1.2 \times 10^{-12} \quad (31)$$

and

$$|\bar{g}_{\pi nn}^{(1)}| < 1.1 \times 10^{-12}. \quad (32)$$

The $\bar{\theta}$ scenario offers $\bar{g}_{\pi nn}^{(0)} = (-0.018 \pm 0.007)\bar{\theta}$ and $\bar{g}_{\pi nn}^{(1)} = (0.003 \pm 0.002)\bar{\theta}$ [34, 35]. This results in the best limit on $\bar{\theta}$ as [34]

$$|\bar{\theta}| < 1.1 \times 10^{-10}. \quad (33)$$

Also using the limit on $\bar{g}_{\pi nn}^{(1)}$ and the relation from the the minimal supersymmetric left-right model as $\bar{g}_{\pi nn}^{(1)} = 2 \times 10^{-12} \times (\tilde{d}_u - \tilde{d}_d)$ [23, 42], we can give

$$|\tilde{d}_u - \tilde{d}_d| < 5.5 \times 10^{-27} |e|\text{cm}. \quad (34)$$

All the above limits can be improved further when more accurate nuclear calculations on a_i and experimental limit on the

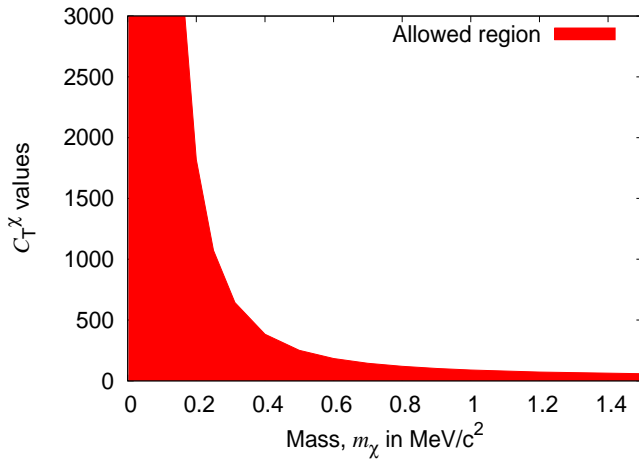


FIG. 4: (Color online) The area shown in color are the allowed region of the C_T^X values with the m_χ values (in MeV/c^2). This range is substantially different than that were estimated in Ref. [36].

EDM of the ^{199}Hg atom are available. The SM offers an open range of value to $\bar{\theta}$ from 0 to 2π , while the above restriction is a clear indication of existence of BSM.

Having discussed on various limits for the infinite m_χ approximation, we turn onto investigating constraint on the T-PT coupling coefficient C_T^X by considering a range of m_χ from the low to intermediate energy scale. In order to validate our method for investigating this quantity, we analyze first the behavior of $\rho_N^X(r)$ against the radial distance r from the origin of the nucleus and compare with its trend for the given values of m_χ as plotted in Ref. [36]. These trends are shown in Fig. 1 and we find that it reproduces the same trends as in Ref. [36]. It indicates that we have constructed $\rho_N^X(r)$ properly. Earlier, we have also demonstrated as our RPA calculations agree with the RPA results reported in Ref. [38]. From this analysis, we anticipate to reproduce the DHF and RPA results of Ref. [36] and would like to demonstrate the results using the CCSD method.

In Table II, we list the d_a^X values by considering a wide range of m_χ values from the DHF, RPA and CCSD methods. As can be seen, the difference between the RPA and CCSD results are quite significant for all the values of m_χ . We have also given values for $m_\chi = \infty$. It can be noticed that these values are almost similar to that are given in Table I, but the slight differences are owing to the consideration of the uniform nuclear charge distribution than the earlier considered Fermi nuclear charge distribution in the evaluation of $\rho_N^X(r)$. Again as were mentioned before due to the large cancellation between the all order electron core-polarization and pair-correlation effects in the CCSD method, the CCSD values are coming out to be more close to the DHF values than the RPA values. In fact, we highlight these differences by plotting the d_a^X values for different range of m_χ values in Figs. 2. This plot clearly shows how RPA overestimates the electron correlation effects in the ^{199}Hg atom. Thus, RPA does not seem to be suitable to employ for precise determination of constraints on the C_T^X values though it accounts electron correlations due to core-polarization effects to all orders; rather it would be more appropriate to use results from the DHF method as an effortless method for more valid estimate

of C_T^X values. Considering these results, we also determine \mathcal{R}^X values from all the employed methods and plot them in Fig. 3. Interestingly, it can be noticed from this figure that the obtained \mathcal{R}^X values from all the employed methods agree quite well with each other irrespective of the fact that inclusion of the electron correlation effects change the d_a^X values substantially from the DHF method. However, zooming the plots more closely, as shown in the inset of Fig. 3, we find that there are small differences in the \mathcal{R}^X values from all the considered three methods.

After observing that the RPA method is overestimating the electron correlation effects, we consider the CCSD results of \mathcal{R}^X and d_a^X/C_T to infer constraint on C_T^X . Though we find \mathcal{R}^X values do not change much even with the inclusion of the electron correlation effects, but it can be seen from Table II that the C_T value differs significantly among the methods employed here. From Eq. (16), it is obvious that limit on C_T^X depends on both the \mathcal{R}^X and C_T values, therefore it is still upholds our argument to consider a valid method to evaluate limit on C_T^X more precisely. By combining these \mathcal{R}^X and C_T values from the CCSD method for a range of m_χ with the experimental limit $|d(^{199}\text{Hg})| < 7.4 \times 10^{-30} \text{ ecm}$ with 95% confidence level [10], we estimate the limits on the C_T^X values and plot them in Fig. 4. The area shown in color in this figure is the allowed region for the C_T^X for all the considered masses of a possible dark matter candidate χ . If the EDM of the ^{199}Hg atom is ascertain in future then C_T^X can be found out, from which we expect to determine m_χ value precisely.

V. CONCLUSION

We have investigated limits on the tensor-pseudotensor and scalar-pseudoscalar coupling coefficients of the electron-nucleus interactions due to parity and time-reversal symmetry violations. Limits on the CP violating quantum chromodynamics parameter $\bar{\theta}$ and chromo-electric dipole moments of quarks were evaluated from the limits obtained on the nuclear Schiff moment. To determine these limits, we have combined the recently reported experimental limit on the electric dipole moment of the ^{199}Hg atom with the sophisticated atomic calculations carried out based on the relativistic many-body methods. We observed from the comparison among the atomic results obtained by employing methods in the random phase approximation and coupled-cluster theory framework that choice of a suitable atomic many-body method plays crucial roles in accounting the electron correlation effects rigorously for accurate determination of the above limits at the cost of large computation. Further, allowing Yukawa-type parity and time-reversal symmetry violating interactions between the electrons and nucleus in the ^{199}Hg atom due to a plausible dark force carrier χ , constraints on the values of the tensor-pseudotensor coupling coefficient for a wide range of mass of χ have been imposed.

Acknowledgement

This work was partly supported by the TDP project of Physical Research Laboratory (PRL), Ahmedabad and the computations were carried out using the Vikram-100 HPC cluster of PRL.

-
- [1] N. F. Ramsey, Ann. Rev. Nucl. Part. Sci. **32**, 211 (1982).
 - [2] L. D. Landau, Sov. Phys. JETP **5**, 336 (1957).
 - [3] N. Fortson, P. Sandars, and S. Barr, Phys. Today, pg. 33, June (2003).
 - [4] G. Liders, Ann. Phys. (N.Y.) **281**, 1004 (2000).
 - [5] I. B. Khriplovich and S. K. Lamoreaux, *CP violation without strangeness. Electric dipole moments of particles, atoms, and molecules*, (Springer, Berlin, 1997).
 - [6] B. L. Roberts and W. J. Marciano, *Lepton Dipole Moments, Advanced series on Directions in High Energy Physics*, vol. 20, World Scientific, Singapore (2010).
 - [7] C. A. Baker et al, Phys. Rev. Lett. **97**, 131801 (2006).
 - [8] J. J. Hudson et al, Nature **473**, 493 (2011).
 - [9] J. Baron et al, Science **343**, 269 (2014).
 - [10] B. Graner, Y. Chen, E.G. Lindahl, and B.R. Heckel, Phys. Rev. Lett. **116**, 161601 (2016).
 - [11] M. Bishof, R. H. Parker, K. G. Bailey, J. P. Greene, R. J. Holt, M. R. Kalita, W. Korsch, N. D. Lemke, Z. T. Lu, P. Mueller, T. P. OConnor, J. T. Singh and M. R. Dietrich, Phys. Rev. C **94**, 025501 (2016).
 - [12] J. H. Christenson, J. W. Cronin, V. L. Fitch, and R. Turlay, Phys. Rev. Lett. **13**, 138 (1964).
 - [13] K. Abe et al., Phys. Rev. Lett. **87**, 091802 (2001).
 - [14] B. Aubert et al., Phys. Rev. Lett. **87**, 091801 (2001).
 - [15] R. Aaij et al., Phys. Rev. Lett. **110**, 221601 (2013).
 - [16] M. J. Ramsey-Musolf and S. Su, Phys. Rep. **456**, 1 (2008).
 - [17] S. M. Barr, Int. J. Mod. Phys. A **8**, 209 (1993).
 - [18] M. Pospelov and A. Ritz, Ann. Phys. (N.Y.) **318**, 119 (2005).
 - [19] M. Dine and A. Kusenko, Rev. Mod. Phys. **76**, 1 (2003).
 - [20] L. Canetti, M. Drewes and M. Shaposhnikov, New J. Phys. **14**, 095012 (2012).
 - [21] T. Fukuyama, Int. J. Mod. Phys. A **27**, 1230015 (2012).
 - [22] S. M. Barr, Phys. Rev. D **45**, 4148 (1992).
 - [23] M. Pospelov, Phys. Lett. B **530**, 123 (2002).
 - [24] J. Engel, M. J. Ramsey-Musolf, and U. van Kolck, Prog. Part. Nuc. Phys. **71**, 21 (2013).
 - [25] P. G. H. Sandars, Phys. Lett. **14**, 194 (1965).
 - [26] J. S. M. Ginges and V. V. Flambaum, Phys. Rep. **637**, 63 (2004).
 - [27] A. M. Maartensson-Pendrill, Phys. Rev. Lett. **54**, 1153 (1985).
 - [28] V. F. Dmitriev and R. A. Senkov, Phys. Rev. Lett. **91**, 21 (2003).
 - [29] J. M. Pendelbury et al., Phys. Rev. D **92**, 092003 (2015).
 - [30] M. A. Rosenberry and T. E. Chupp, Phys. Rev. Lett. **86**, 31 (2001).
 - [31] W. C. Griffith et al., Phys. Rev. Lett. **102**, 101601 (2009).
 - [32] R. H. Parker, et al., Phys. Rev. Lett. **114**, 233002 (2015).
 - [33] Y. Singh and B. K. Sahoo, Phys. Rev. A **91**, 030501(R) (2015).
 - [34] W. Dekens et al., JHEP **1407**, 069 (2014).
 - [35] J. de Vries, E. Mereghetti, and A. Walker-Loud, Phys. Rev. C **92**, 045201 (2015).
 - [36] H. Gharibnejad and A. Derevianko, Phys. Rev. D **91**, 035007 (2015).
 - [37] I. Shavitt and R. J. Bartlett, *Many-body methods in Chemistry and Physics*, Cambridge University Press, Cambridge, UK (2009).
 - [38] V. A. Dzuba, V. V. Flambaum and S.G. Porsev, Phys. Rev. A **80**, 032120 (2009).
 - [39] B. K. Singh, Y. Singh and B. P. Das, Phys. Rev. A **90**, 050501(R) (2014).
 - [40] Y. Singh and B. K. Sahoo, Phys. Rev. A **92**, 022502 (2015).
 - [41] D. Goebel and U. Hohm, J. Phys. Chem. **100**, 7710 (1996).
 - [42] J. Bsaisou et al, Eur. Phys. J. A **49**, 31 (2013).